Observations on rotating needle insertions using a brachytherapy robot

2007 Phys. Med. Biol. 52 6027

(http://iopscience.iop.org/0031-9155/52/19/021)

IOP PUBLISHING PHYSICS IN MEDICINE AND BIOLOGY

Phys. Med. Biol. **52** (2007) 6027–6037 doi:10.1088/0031-9155/52/19/021

Observations on rotating needle insertions using a brachytherapy robot

M A Meltsner[1], N J Ferrier[2] and B R Thomadsen[1,3]

[1] Department of Medical Physics, University of Wisconsin, Madison, WI 53706, USA
[2] Department of Mechanical Engineering, University of Wisconsin, Madison, WI 53706, USA
[3] Departments of Human Oncology, Biomedical Engineering and Engineering Physics, University of Wisconsin, Madison, WI 53706, USA

Received 30 May 2007, in final form 20 August 2007
Published 17 September 2007
Online at stacks.iop.org/PMB/52/6027

Abstract

A robot designed for prostate brachytherapy implantations has the potential to greatly improve treatment success. Much of the research in robotic surgery focuses on measuring accuracy. However, there exist many factors that must be optimized before an analysis of needle placement accuracy can be determined. Some of these parameters include choice of the needle type, insertion velocity, usefulness of the rotating needle and rotation speed. These parameters may affect the force at which the needle interacts with the tissue. A reduction in force has been shown to decrease the compression of the prostate and potentially increase the accuracy of seed position. Rotating the needle as it is inserted may reduce frictional forces while increasing accuracy. However, needle rotations are considered to increase tissue damage due to the drilling nature of the insertion. We explore many of the factors involved in optimizing a brachytherapy robot, and the potential effects each parameter may have on the procedure. We also investigate the interaction of rotating needles in gel and suggest the rotate-cannula-only method of conical needle insertion to minimize any tissue damage while still maintaining the benefits of reduced force and increased accuracy.

1. Introduction

1.1. Background

Prostate cancer is the most frequently diagnosed non-skin cancer among men in the United States (Jemal *et al* 2005). Over the past decade, brachytherapy has become an increasingly popular treatment for prostate cancer when detected in the early stages. Alternatives to brachytherapy include radical prostatectomy or external beam radiation treatments (EBRT) using a linear accelerator. A combination of brachytherapy and EBRT is commonly performed when the patient is considered to be at a risk for extraprostatic disease (Ragde *et al* 1998). Brachytherapy alone (monotherapy) has been shown to be comparable in cost to radical

prostatectomy with a similar quality of life assessments (Makhlouf *et al* 2002, Krupski *et al* 2000). Brachytherapy maintains an advantage in the duration of treatment compared with EBRT and reduced invasiveness compared with surgery while providing similar or better prostatic specific antigen (PSA) control rates to both modalities (Ragde *et al* 1998, Yu *et al* 1999).

The most common method for interstitial prostate brachytherapy is the transperineal deposition of low-dose rate ^{103}Pd, ^{125}I or ^{131}Cs sources within the organ. The sources typically are deposited by one of two methods: (1) hollow, pre-loaded, bevel-tipped needles or (2) diamond- or conical-tipped stylets within a cannula with subsequent retraction of the stylet and injection of the sources using a device such as the MICK® applicator (Mick Radionuclear, Mount Vernon, NY, USA). Both methods utilize trans-rectal ultrasound (TRUS) to guide the needle. The needle is inserted perpendicularly through a 0.5 cm spaced, template grid placed against the perineum (Yu *et al* 1999, Berkeley 1994)

The use of a template grid to guide needle insertions for low-dose-rate (LDR) brachytherapy may limit the efficacy of the procedure. Ideal locations for needle insertion may not fall into the 0.5 cm constraint. Additionally, the prostate may be shadowed by the pubic arch. Patients with pubic arch interference (PAI) or overly large prostates may receive inadequate coverage of the tumor due to the perpendicular-only insertion of needles required by the template in the TRUS procedure (Yu *et al* 1999).

The quality of life in a brachytherapy patient may be significantly affected due to the lack of accuracy associated with the procedure (Dawson *et al* 1994). Some of the more common negative responses may include: erectile dysfunction, urinary and bowel incontinence, rectal bleeding and diarrhea (Krupski *et al* 2000, Merrick *et al* 2000). Ankem *et al* (2002) determined in a 58 patient study that 36.2% of prostate brachytherapy procedures have at least one source migrate to the chest cavity. Lee *et al* (2000) found that 12% of patients required a catheter to relieve urinary obstruction after LDR prostate brachytherapy. The outcome for the patient is dependent on the accuracy of the source distribution, edema due to needle insertion and doses to the urethra and rectum.

Several robots have been developed specifically for prostate brachytherapy (Ng *et al* 1996, Fichtinger *et al* 2001, Wan *et al* 2005, Yu *et al* 2006). Each robot's unique characteristics can benefit LDR prostate brachytherapy by potentially increasing accuracy of needle placement, reducing edema and swelling resulting in better post-implant results.

The recent development of a 'directional' source has further necessitated the use of robots in prostate brachytherapy (Lin *et al* 2006). A directional source is similar to a conventional brachytherapy source; however one side of the jacket is shielded, thus blocking radiation on that side of a normally isotropic source. The potential to shield the urethra and rectum, as well as reduce radiation 'hot-spots' within the prostate proper are just some of the potential benefits of this source. The effectiveness of the source is extremely sensitive to rotational effects. A robot is necessary not only to implant these sources, but also to orient them accurately around the source axis ensuring that the source irradiates the proper structures.

1.2. Effects of needle rotations

Wan *et al* (2005) showed that rotating a bevel needle at 4 rev s^{-1} as it is inserted reduces the displacement from the target position compared to stationary insertions. They concluded that constant rotation of the needle as it is inserted would be prohibitive due to the drilling nature of the insertion which would increase tissue damage, though the accuracy of the needle tip would be increased over stationary or the 'orientation reversal method,' in which the needle is rotated 180° at half the distance to the target.

The present work examined the effect of needle rotation on gel and beef phantoms with different rotational speeds for both beveled and conical needles, with a focus on tissue damage and insertion force requirements. Furthermore, the investigation considered the effect of needle type, insertion velocity, needle rotation necessity and insertion force values on a robotic brachytherapy implantation.

2. Materials and methods

2.1. Brachytherapy robot

The prototype robot is a six degree-of-freedom (DOF) manipulator, comprised of three linear motorized slides and two rotary motorized stages. The sixth DOF is the motorized rotation of the needle along its axis. Each of the three linear slides is a Parker–Hannifin® (PH) (Parker, Rohnert Park, CA, USA) 250 mm travel 404XR with a linear screw drive with a pitch of 1 mm rev^{-1}. One of the rotary stages is a PH 250 mm diameter 200RT table while the second rotary stage is a PH 150 mm diameter 200RT table. Each stage is powered by a servo motor, which is set to have a resolution of 4000 counts rev^{-1} with the feedback mechanism ensuring a powered position accuracy of ± 1 count. The theoretical accuracy of the linear stages is 0.000 25 mm. The theoretical accuracy of the rotary stages is 0.0005°.

Figure 1 shows the design of the robot attached to the underside of a table (figure 1(b)) and a mobile cart (figure 1(c)). The robot was moved from the fixed position on the underside of the table to a wheeled cart for added mobility in the operating room. The first linear slide is mounted horizontally and provides movements in the x-direction (left-and-right). The second linear slide is mounted at a 90° angle to the first slide with a 90° mounting bracket manufactured by PH. This slide moves the robot in the y-direction (up-and-down). The 250 mm rotary table is attached to the y-slide, and provides rotations around the x-axis (roll). A custom mounting plate is attached to the 250 mm and 150 mm rotary tables at a 180° orientation to the y-slide. The 150 mm rotary table rotates around the y-axis (pitch). Due to the constraints of the workspace, the two rotary tables are confined to $\pm 30°$ of movement from perpendicular. The robot utilizes angled insertions to avoid the problems of PAI, which the perpendicular-only nature of the standard TRUS method limits (Yu *et al* 1999). Angulation also allows flexibility in minimizing the number of needle tracks for a seed location pattern.

Mounted on the 150 mm rotary table is the third 404XR linear slide. This slide moves along the z-direction and is responsible for needle insertion. On top of the z-slide, two linear ball-bearing and rail combinations allow a block to slide freely along the z-axis. This block assembly is necessary to decouple the insertion movement from automatic motion if desired. The movement in the insertion direction is selectable between automatic (motor-controlled) and manual (human-controlled). This is a convenience for the physician if one feels uncomfortable with automatic insertions. The sliding assembly can be locked in place to ensure stable, automatic insertion. From the block, an aluminum arm extends upward 0.38 m. Attached at the top of this arm is the final motor and gearing mechanism for the ability to rotate the needle along its axis (yaw). An automatic seed loading mechanism is being designed to deposit the sources in the tissue after the needle has been inserted. In the case of conical needles, the stylet retracts and the directional or conventional sources are pushed down the cannula into the tissue.

The robot is controlled through a graphical user interface (GUI) custom written for controlling the device. The standard language included with the PH Gemini™ (Parker, Rohnert Park, CA, USA) servo drive/controllers was used as a basis and programmed into the GUI using Visual Basic 6™ (Microsoft, Seattle, USA). A Pentium M 1.6 GHz laptop was

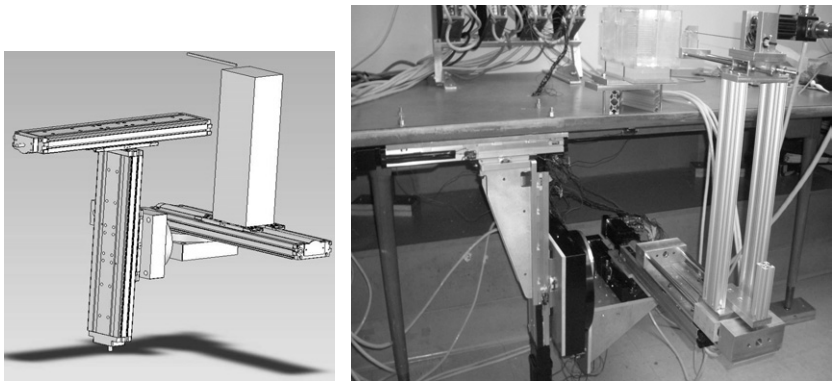

(a) (b)

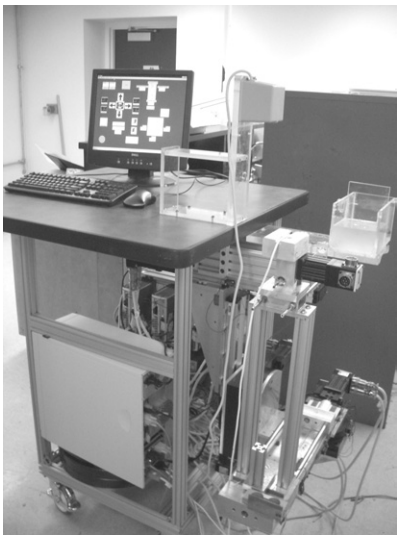

(c)

Figure 1. The brachytherapy robot (a) simplified schematic, (b) prototype attached to a table and (c) prototype on a mobile cart.

connected through a serial cable to the robot and an HP 34401A multimeter. The multimeter measured the voltage of the force-sensing strain gauge. The serial connections to both the multimeter and robot limit the sampling rate of voltage information from the strain gauge and robot position from the servo drivers. For this reason, the speed of the robot in force measurements is limited to 20 mm s^{-1}, although the robot is capable of insertion speeds up to 70 mm s^{-1} in its current configuration. Future iterations of the device will reach greater velocities while using an interface other than serial to access information faster.

2.2. Needle choice

The two types of needles explored in this investigation were hollow 30 cm, 17 gauge, bevel-tipped needles and 17 gauge, 30 cm conical-tipped needles (figure 2). Both needles were supplied by BEST Medical® (Springfield, VA, USA). A typical TRUS guided insertion for

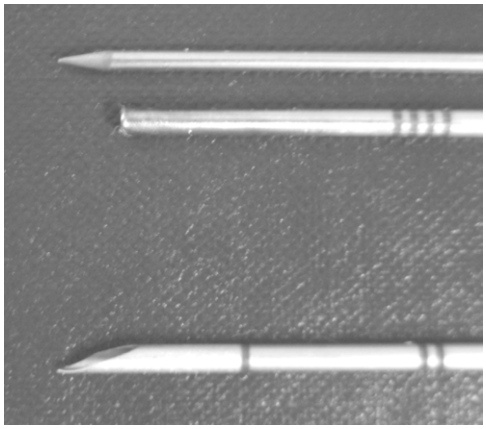

Figure 2. The conical needle with a sharpened stylet and a hollow cannula (top) and a bevel needle (bottom).

low-dose rate brachytherapy utilizes 20–25 cm 18 gauge needles with either a bevel tip or a conical- or diamond-tipped stylet with hollow cannula combination. The robot requires a longer needle to allow for attachment to the gearing mechanism in the sixth DOF, which would not leave enough length to reach the prostate if longer needles were not used. BEST medical did not manufacture 30 cm, 18 gauge needles; however 17 gauge needles were available in that length. For consistency, the comparison used the 17-gauge conical-tipped needles as well.

2.3. Phantom design

Two phantoms were used to determine optimal insertion factors: a gel phantom for force measurements and damage comparisons, and a beef phantom for force measurements. The initial experiments required a homogenous material through which the needles could be inserted. The gel material provided an adjustable, clear solution.

A key characteristic of using gel is that one can easily alter the formula to achieve different Young's moduli. Krouskop *et al* (1998) measured Young's moduli of several tissues within the body. A cancerous prostate had a value of 96 kPa which is nearly twice the value of the normal, anterior prostate (55 kPa) at 2% precompression and 0.1 Hz loading frequency. Most other tissues, such as fat and connective tissues, have significantly lower values than 55 kPa, however. An EnduraTec model 3200 ELF (Bose Corporation, ElectroForce Systems Group, Eden Prarie, MN, USA) dynamic testing system measured Young's modulus of a 12% gel mixture to be 47 kPa. This value is in the range of many tissues within the body (between 10 kPa and over 100 kPa) and is particularly close to the value for the normal prostate (DiMaio and Salcudean 2003, Krouskop *et al* 1998). Thus, this mixture of gel was determined to be optimal for simulating needle interactions with most tissues.

The gel used in this experiment consisted of 300 bloom strength porcine gelatin in a 12% mixture with de-ionized water. After 1 h of settling time, the gel mixture was heated to 55–60 °C until the mixture turned clear. The mixture was poured into the acrylic phantom and placed in a refrigerator overnight. The morning of the experiment, the gel was left to warm at room temperature for several hours before needle implantation experiments began. Figure 3 shows the acrylic phantom with the solid gel in relation to the robot and needle guide.

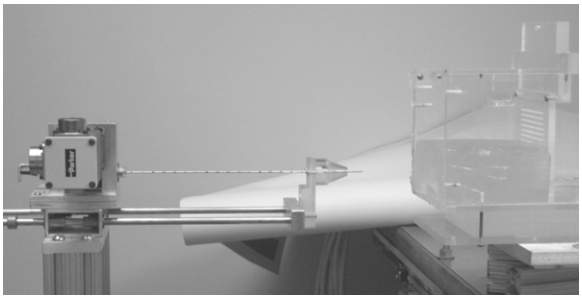

Figure 3. The robot needle guide approaching gel phantom in an acrylic holder.

2.4. Force measurements

The following experiments sought to compare the force necessary for the robot to maintain the set speed as each type of needles was inserted. Several researchers have investigated needle insertion forces (O'Leary *et al* 2003, Okamura *et al* 2004, Podder *et al* 2005, DiMaio and Salcudean 2003). Here, we compare the force requirements for both the bevel and conical needle types with and without rotation in the gel phantom. In addition, we repeated the experiment using two pieces of eye of round beef from a local butcher. The beef does not provide a homogenous medium but gives a general 'feel' of human tissue.

Force measurements were performed with a calibrated, one-dimensional 3 kg load cell (Elane Electronics, China). The gauge was calibrated from 0 to 2 kg and was shown to be extremely linear. The conversion from voltage to equivalent force was determined in this calibration step. The scale was attached to the robot at the base of the extending arm at the end of the sliding block. As the needle is inserted, force is applied at the needle tip. Force is also applied at the base where the unlocked block pushes against the strain gauge. The resulting output force is sampled with a HP 34401A multimeter.

2.5. Damage assessment

In addition to its benefit of homogeneity, gel is an effective comparison medium in which to observe tissue damage potential. The clear gel allows for the visual inspection of the needle interaction. This is important to assess the tissue damage potential for different combinations of insertion parameters, including rotation during insertion.

3. Results

3.1. Force measurements

Force versus insertion depth for conical and bevel needles in gel and beef is plotted in figure 4. Each plot is a cubic-spline average of multiple insertions, except in figure 4(d) in which each data set is based on a single insertion. Figures 4(a) and (b) were performed on the same day in the same phantom. Figure 4(d) is the result of another experiment in a similarly formulated gel phantom. This, combined with the lack of splined averaging, may explain the small disparity in force requirements for similar insertion parameters compared to figure 4(a). Figure 4(c) is the combination of data from two pieces of similar cuts of beef.

There is little difference in force requirements between stationary bevel and conical needles at slower speeds (figure 4(b)). However, there appears to be a separation emerging when speeds are increased to above 20 mm s^{-1}. O'Leary *et al* (2003) found that bevel needles in general have a lower resistive force than conical tips.

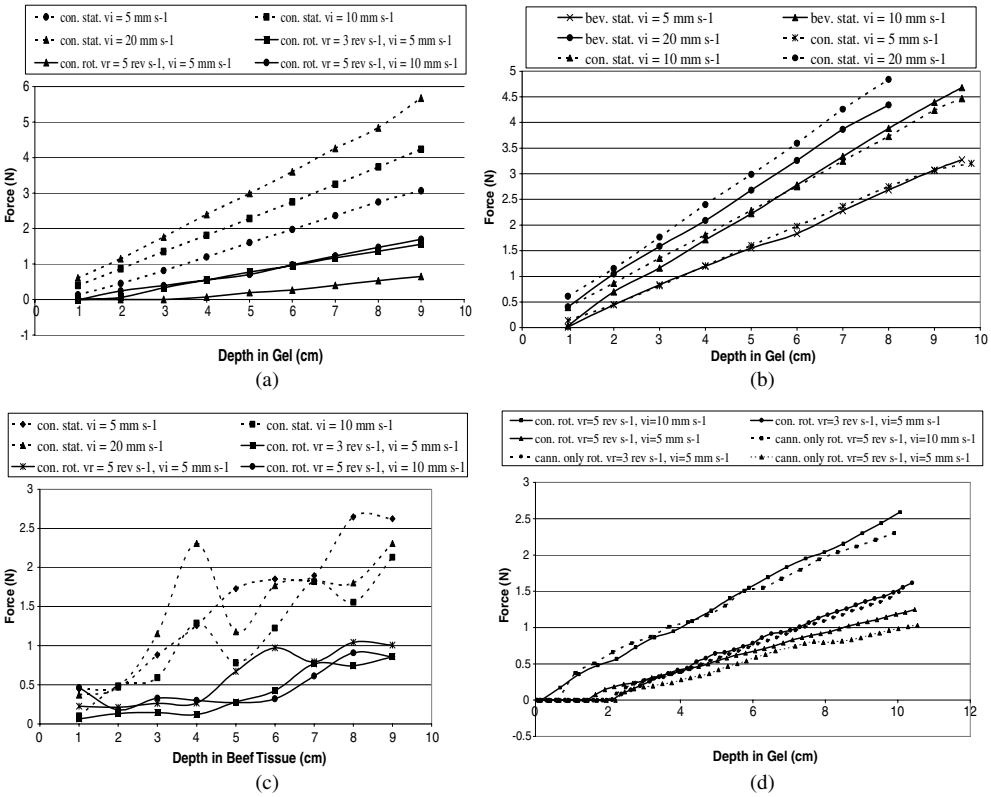

Figure 4. Needle force data at 5, 10 and 20 mm s^{-1} insertion speed: (a) comparison between stationary and select rotated complete conical insertions in gel, (b) comparison between bevel needle and conical needle stationary insertions in gel, (c) comparison of stationary versus select rotated conical insertions in beef, (d) complete conical needle rotation versus cannula only method in gel.

Three combinations of rotation speed and insertion velocity consistently demonstrated significantly reduced force requirements. These three combinations were: (1) $v_r = 3$ rev s^{-1}, $v_i = 5$ mm s^{-1}, (2) $v_r = 5$ rev s^{-1}, $v_i = 5$ mm s^{-1} and (3) $v_r = 5$ rev s^{-1}, $v_i = 10$ mm s^{-1}, where v_r is the speed of rotation and v_i is the speed of insertion. A comparison of these three rotated insertions in gel versus their stationary counterparts for the conical needles is plotted in figure 4(a). The lowest force requirements were in the $v_r = 5$ rev s^{-1}, $v_i = 5$ mm s^{-1} insertion. At 9 cm depth, the force of insertion at $v_r = 5$ rev s^{-1}, $v_i = 5$ mm s^{-1} was 0.65 N compared to the maximum measured value of 5.7 N for the $v_i = 20$ mm s^{-1} stationary insertion and 3.1 N for the $v_i = 5$ mm s^{-1} stationary insertion. This is a reduction of 89% and 79%, respectively. A comparison in beef is plotted in figure 4(c). Similar trends are seen here, though the inhomogenous nature of the material lends to nonlinear results, even with the cubic-spline averaging. Still, a reduction in force of greater than 50% can be seen.

3.2. Damage considerations for rotated insertions

The damage done to tissue by the rotation of the needle is a concern and may outweigh any potential benefits unless a compromise can be found. Lee *et al* (2000) posited that greater edema due to increased needle punctures contributed to urinary retention in LDR

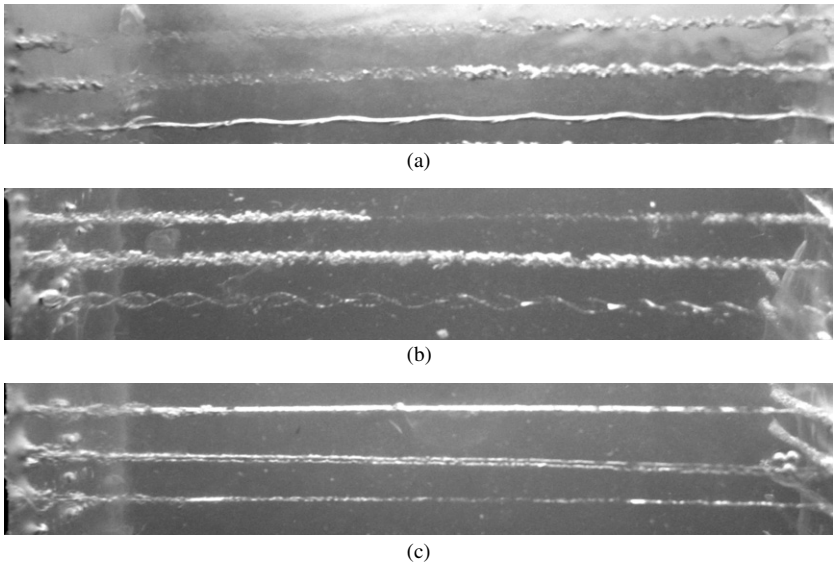

Figure 5. Photographs of the damage done by rotating the (a) bevel needle, (b) complete conical needle and (c) cannula only of the conical needle at three rotation speeds, v_r, of 1, 3, 5 rev s^{-1} in increasing order from the bottom to top of each image. Insertion speed, v_i, was constant at 10 mm s^{-1}. Pictures are in the same scale.

brachytherapy patients. Figures 5(a) and (b) show a comparison of the tissue damage by each needle when rotated at different speeds. For the bevel and complete conical rotations, a spiral track is seen at slower rotation speeds. As the rotation speed is increased, the damage to the gel becomes greater, with the displaced fragments becoming more refined for both the conical needle and bevel needle. An increase in tissue damage will increase swelling and bleeding and may not provide a beneficial outcome to the patient even with the potential increases in needle accuracy and source placement inherent in robotic surgery.

The robot is designed so that the cannula may rotate separately from the conical, cutting stylet (figure 7). Figure 5(c) demonstrates the reduction of damage along the insertion track when only the cannula rotates. The track diameter appears smaller than the other rotated insertions, and there is little fragmentation visible in the gel. The cutting tip is stationary, so no damage from the spiraling of the tip occurs as seen in figures 5(a) and (b). Figure 6 displays an insertion in which dye enhances the contrast of the insertion track against the background of the gel. The rotate-cannula-only (RCO) method has a similar track outline to a stationary needle insertion. It is important to note that the darkness of the track is proportional to the amount of dye that was released into the track as the needles were retracted. This was not constant throughout the experiment, but the dye promotes comparison between stationary and rotated insertions.

3.3. Force reduction

The (RCO) method has the benefit of reducing friction (and thus insertion force) over a stationary insertion while not contributing to large increases in tissue damage as does a complete conical or bevel rotated insertion. Figure 4(d) shows that the force required for the RCO insertion is similar to the complete conical needle rotated insertion. This suggests that the bulk of the force is due to friction along the cannula shaft, which decreases with rotation.

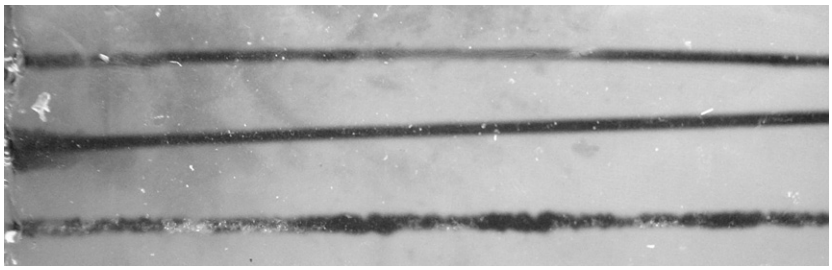

(a)

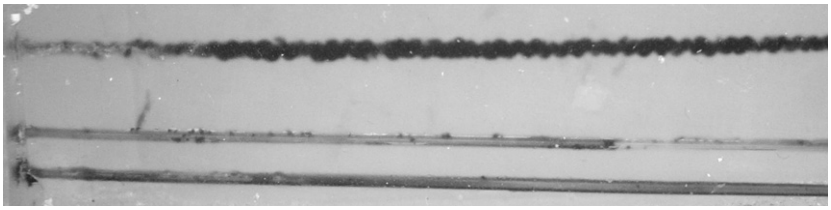

(b)

Figure 6. Images of needle interaction with gel, enhanced with dye left in track during retraction. All insertions are with $v_i = 10$ mm s^{-1}. (a) top: a $v_r = 5$ rev s^{-1} RCO needle insertion; middle: a stationary conical needle insertion; and bottom: a complete conical needle rotated at $v_r = 5$ rev s^{-1}. (b) top: a bevel needle rotated at $v_r = 5$ rev s^{-1}; middle: a stationary bevel insertion; and bottom: another bevel stationary insertion using slightly more dye than in (b) middle.

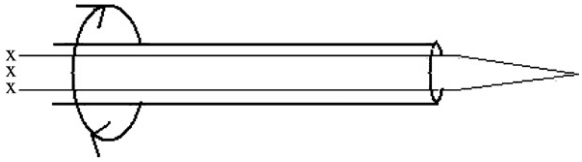

Figure 7. A diagram of the RCO method of conical needle rotation. The cannula is rotated while the conical cutting stylet is held stationary, resulting in less damage during insertion.

There is good evidence to suggest that rotating the needle, with resulting reduction of force, will increase the accuracy of *source* placement by reducing the compression of tissues. Alterovitz *et al* (2003) performed a series of finite element analyses (FEA) on prostate compression due to needle insertion. They explored the effects of different variables on the insertion, including force. While the tip of the needle may find its target position accurately within the space of the prostate, the compression of the prostate and its resulting decompression when the needle is removed causes the source to end as much as 20% of the width of the prostate from its intended target. In some cases, this error can be accounted for in the treatment planning software. This becomes problematic, however, near the internal edges of the prostate where insertion beyond the intended position is not feasible. In addition, parameters such as tissue inhomogeneity can reduce the efficacy of software corrections. A reduction in the frictional force as the needle is inserted can reduce the compression of the prostate with a subsequent increase in source deposition accuracy (Alterovitz *et al* 2003). Furthermore, Lagerburg *et al* (2006) found that tapping the prostate in a high-speed (maximum 31 m s^{-1}), repetitive insertion can reduce the motion of the prostate as the needle reaches the desired depth. The high velocity tapping reduces the kinetic friction of the needle. Rotating the needle

during insertion can reduce frictional forces and perhaps minimize prostate motion in addition to compression.

4. Conclusions and future work

The robotic system has great potential to increase not only the needle placement accuracy but also the source deposition accuracy for prostate brachytherapy. The rotation of the conical needle may reduce frictional forces and create less compression and prostate motion leading to more accurate implantations. The rotate-cannula-only method provides this decrease in insertion force with minimal increases in tissue damage. Future work would analyze similar characteristics of the triangular pyramid, or diamond-tipped needle to the conical needle. Okamura *et al* (2004) found that this needle had the lowest resistive forces of the three types of needles.

A balance exists between the insertion and rotation velocities to minimize tissue damage and maintain implant accuracy. A faster insertion velocity may increase force, but may also reduce tissue damage at a set rotation speed because of a decrease in the number of rotations per needle track. It is hypothesized that the optimal implant would be a combination of stationary and rotated insertions with varying velocities along the needle path. Future work will explore these parameters with pig prostates.

With the advent of directional sources, every advantage must be taken to ensure the proper placement and orientation of these sources. Small deviations in prescribed positions can prevent an optimal result. The work presented here aids in the initial placement of the source. Future work will research the most favorable method to ensure stability of the directional source in position and orientation post-implantation. A robot is the best method by which directional (and conventional) sources may be localized for prostate brachytherapy, leading to the most conformal implantation possible and better outcomes for more patients.

References

Alterovitz R, Goldberg K, Pouliot J, Taschereau R and Hsu I 2003 Needle insertion and radioactive seed implantation in human tissues: simulation and sensitivity analysis *Proc. 2003 IEEE Int. Conf. on Robotics and Automation (Taipei, Taiwan)* pp 1793–9

Ankem M K *et al* 2002 Implications of radioactive seed migration to the lungs after prostate brachytherapy *Urology* **59** 555–9

Berkeley L W 1994 Design and treatment planning for permanent implants *Brachytherapy Physics: AAPM Summer School* ed J F Williamson, B R Thomadsen and R Nath (Madison, WI: Medical Physics Publishing) pp 427–38

Dawson J E, Wu T, Roy T, Gy J Y and Kim H 1994 Dose effects of seed placement deviations from pre-planned positions in ultrasound guided prostate implants *Radiother. Oncol.* **32** 268–70

DiMaio S P and Salcudean S E 2003 Needle insertion modeling and simulation *IEEE Trans. Robot. Autom.* **19** 864–74

Fichtinger G, Masamune K, Patriciu A, Tanacs A, Anderson J H, DeWeese T L, Taylor R H and Stoianovic D 2001 Robotically assisted percutaneous local therapy and biopsy *Workshop Proc. 10th IEEE Int. Conf. of Advance Robotics (Budapest, Hungary)* pp 133–51

Jemal A, Murray T, Ward E, Samuels A, Tiwari R C, Ghafoor A, Feuer E J and Thun M J 2005 Cancer statistics *CA Cancer J. Clin.* **55** 10–30

Krouskop T A, Wheeler T M, Kallel F, Garra B S and Hall T 1998 Elastic moduli of breast and prostate tissues under compression *Ultrason. Imaging* **20** 269–70

Krupski T, Petroni G R, Bissonette E A and Theodorescu D 2000 Quality of life comparison of radical prostatectomy and interstitial brachytherapy in the treatment of clinically localized prostate cancer *Urology* **55** 737–42

Lagerburg V, Moerland M A, Konings M K, van de Vosse R E, Lagendijk J J W and Battermann J J 2006 Development of a tapping device: a new needle insertion method for prostate rachytherapy *Phys. Med. Biol.* **51** 891–902

Lee N, Wuu C S, Brody R, Laguna J L, Katz A E, Bagiella E and Ennis R 2000 Factors predicting for postimplantation urinary retention after permanent prostate brachytherapy *Int. J. Radiat. Oncol. Biol. Phys.* **48** 1457–60

Lin L, Chaswal V, Henderson D L and Thomadsen B R 2005 Assessment of a prostate treatment plan using directional brachytherapy sources *Med. Phys.* **32** 2098

Makhlouf A A, Boyd J C, Chapman T N and Theodorescu D 2002 Perioperative costs and charges of prostate brachytherapy and prostatectomy *Urology* **60** 656–60

Merrick G S, Butler W M, Dorsey A T, Galbreath R W, Blatt H and Lief J H 2000 Rectal function following prostate brachytherapy *Int. J. Radiat. Oncol. Biol. Phys.* **48** 667–74

Ng W S, Chung V R, Vasan S and Lim P 1996 Robotic radiation seed implantation for prostatic cancer *18th Ann. Int. Conf. IEEE Eng. in Med. Biol. Society (Amsterdam)* pp 231–3

Okamura A M, Simone C and O'Leary M D 2004 Force modeling for needle insertion into soft tissue *IEEE Trans. Biomed. Eng.* **51** 1707–15

O'Leary M D, Simone C, Washio T, Yoshinaka K and Okamura A M 2003 Robotic needle insertion: effects of friction and needle geometry *Proc. 2003 IEEE Int. Conf. on Robotics and Automation (Taipei, Taiwan)* pp 1774–80

Podder T K *et al* 2005 Evaluation of robotic needle insertion in conjunction with *in vivo* manual insertion in the operating room *IEEE Int. Workshop on Robots and Human Interactive Communication* pp 66–72

Ragde H, Elgamal A A, Snow P B, Brandt J, Bartolucci A A, Nadir B S and Korb L J 1998 Ten-year disease free survival after transperineal sonography-guided Iodine-125 brachytherapy with or without 45-gray external beam irradiation in the treatment of patients with clinically localized, low to high Gleason grade prostate carcinoma *Cancer* **83** 989–1001

Wan G, Wei Z, Gardi L, Downey D B and Fenster A 2005 Brachytherapy needle deflection evaluation and correction *Med. Phys.* **32** 902–9

Yu Y, Anderson L L, Li Z, Mellenberg D E, Nath R, Schell M C, Waterman F M, Wu A and Blasko J C 1999 Permanent prostate seed implant brachytherapy: report of the American association of physicists in medicine task group no. 64 *Med. Phys.* **26** 2054–76

Yu Y *et al* 2006 Robot-assisted prostate brachytherapy *Proc. 2006 Medical Image Computing and Computer-Assisted Intervention Int. Conf. (Copenhagen, Denmark)* pp 41–9